EXPERIMENTAL INVESTIGATION OF CYCLIC AXIAL STRESS-STRAIN RESPONSE OF CFRP-CONFINED CONCRETE

N. Hany[a], E. G. Hantouche[a*], M. H. Harajli[a]

[a] *Department of Civil and Environmental Engineering, American University of Beirut, P.O. Box 11-0236, Riad El-Solh/Beirut 1107 2020, Lebanon, *e-mail: elie.hantouche@aub.edu.lb*

Keywords: Confined concrete columns, Stress-strain response, Carbon fiber reinforced polymer, Cyclic loading.

Abstract

A pilot experimental investigation was carried out for evaluating the stress-strain behavior of carbon fiber reinforced polymer (CFRP) confined plain concrete columns under cyclic compressive loading. The study included 6 specimens of square and circular cross-sections unconfined, partially confined, and fully confined with CFRP. Based on the results of this investigation, the main characteristics of the CFRP confined specimens were identified and existing stress-strain models available in the literature were compared with the experimental results. The results showed that jacketing circular and square specimens with CFRP sheets increases their axial strength, but more importantly leads to substantial increase of the ductility of axial failure. While available models were able to predict the overall trend of the monotonic and cyclic stress-strain response, some discrepancies existed between the models and the characteristic properties of the response. It is anticipated that the data collected from a forthcoming series of tests will lead to the development of a simple and accurate cyclic stress-strain model for CFRP confined concrete.

1. Introduction

Carbon-fiber-reinforced polymer (CFRP) composites are widely used in strengthening and repairing existing reinforced concrete structures due to their effectiveness and ease of installation. Many experimental and analytical investigations have been conducted to evaluate the monotonic and cyclic stress-strain response of concrete columns confined with CFRP laminates. These investigations have clearly demonstrated that confining concrete columns with CFRP jackets leads to substantial improvement of their axial strength, ductility and energy dissipation capacities. Most of the studies have concentrated on FRP-confined concrete specimens subjected to monotonic loading [1-10]. However few investigations have studied the behavior of FRP-confined concrete specimens under cyclic loading [11-21]. Among these studies, the research carried out by Lam and Teng [13] led to the development of a cyclic axial stress-strain model for FRP-confined concrete circular columns. Also, Wang et al. [16, 18] developed two cyclic axial stress-strain models of FRP-confined columns, one for square, and one for circular sections, respectively. An investigation on the influence of the parameters such as confinement level, aspect ratio, concrete strength and corner radius on the behavior of concrete prisms confined with FRP under cyclic loading was carried out by Abbasnia et al. [14, 17, 19, 20]. In this paper, preliminary results from an ongoing

experimental program on CFRP confined concrete specimens of different cross-sectional shapes (circular and square) subjected to cyclic loading are presented to investigate the effects of cross-section geometry and area of CFRP confinement on the cyclic response of concrete columns when confined with CFRP composites. Also, the predictions of three existing cyclic axial stress-strain models proposed by Lam and Teng [13] and Wang et al. [16, 18] are compared with the experimental results.

2. Experimental program

2.1. Test parameters and test specimens

Six plain concrete specimens were fabricated and tested under cyclic axial compression loading. The specimens were divided into three circular specimens of 200 mm diameter and three square specimens of 160 mm side length. All specimens were 500 mm in height. The three specimens in each test series consisted of one unconfined (control) specimen, one specimen wrapped with one layer of discrete CFRP strips having a band width of 50 mm and a clear spacing of 50 mm, and one wrapped with one continuous layer of CFRP applied along the full specimen height. For the square specimens, the corners were rounded to a radius of 10 mm. The specimens are identified in Table 1 with the first letter C and S referring respectively to circular and square cross-sections, while the second letter referring to the wrapping mode, where U stands for unconfined, P for partially confined (using discrete strips) and F for fully confined specimens, respectively. Figure 1 and Table 1 show specimens' details. The concrete mix consisted of coarse aggregate having 10 mm maximum size, natural sand, and Portland cement (Type I), and was proportioned to produce a 28-day cylindrical concrete compressive strength of 20 MPa. The CFRP sheets used were unidirectional, having the following design properties: thickness t_f = 0.13 mm per layer, modulus of elasticity E_{frp} = 230,000 MPa, rupture strain ε_{frp} = 0.015 and ultimate strength f_{fu} = 3500 MPa. Before CFRP application, the surface of the specimens was treated and painted with epoxy resin, and then the CFRP sheets were applied in the transverse direction around the columns with 100 mm overlap. All specimens were capped using a 5 mm thick sulfur layer. The axial strain was measured using two linear variable differential transducers (LVDTs) attached diametrically opposite on the circular specimens, and on opposite sides of the square specimens, over a 250 mm gage length at the middle region of the column as shown in Figure 2. The average strain over the full height of the specimens (gage length = 500 mm) was also measured using two additional LVDTs in the position shown Figure 2. The lateral concrete strain was measured using strain gages mounted on the CFRP sheets at mid-height of the specimens. For the square specimens, the average lateral strain was also measured using two LVDTs attached on either side of the specimens over a gage length of 160 mm. All tests were performed using a 2,000 kN capacity MTS universal testing machine. The specimens were subjected to displacement controlled cycles with three cycles at each displacement level through real test-time LVDT readings.

Specimen	Diameter/ Side Length [mm]	Wrapping	CFRP Width (W) [mm]	Clear Spacing (S) [mm]	ε_{cu} [mm/mm]	f'_{cc} [Mpa]
CU	200	-	-	-	0.0035	11.9
CP	200	Partial	50	50	0.0078	20.12
CF	200	Full	500	0	0.0186	24.15
SU	160	-	-	-	0.00395	5.71
SP	160	Partial	50	50	0.0062	14.62
SF	160	Full	500	0	0.01	18.81

Table 1. Specimen parameters and test results

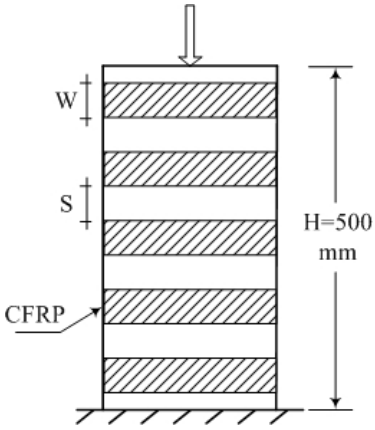

Figure 1. Specimen details: CFRP configuration of partially confined specimens

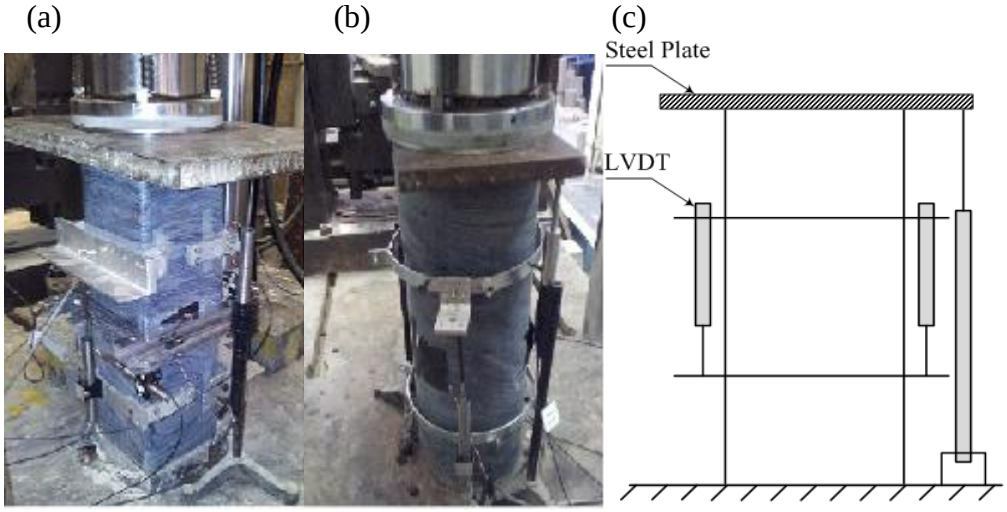

Figure 2. Instrumentation and test set-up: a) Specimen SF - b) Specimen CF - c) LVDTs Configuration.

3. Experimental results

Figures 3(a) and 3(b) show typical failure modes of the confined and the control unconfined specimens, respectively. For the unconfined specimens, failure occurred by complete crushing of concrete as expected. For the confined specimens, failure occurred by sudden rupture of the CFRP sheets which resulted in a sudden drop of load resistance. For the square specimens, the CFRP wraps ruptured at the corners.

Figures 4(a) to 4(b) show the axial stress-strain response for each of the three circular specimens and the three square specimens, respectively.

3.1. Envelope response

Given that all specimens were cast from the same concrete mix, the maximum envelope axial stress attained by the circular unconfined specimen (CU) of 16.6 MPa was smaller (about 90%) than that attained by the square unconfined specimen (SU) of 18.6 MPa, as expected. The peak stress in both unconfined specimens developed at an axial strain very close to 0.002. For the CFRP confined specimens, the envelope stress-strain response is characterized by a three-stage behavior, which is typical of the response of CFRP confined concrete reported in

the technical literature. During the first or elastic stage of the response, at low axial strains and before the CFRP passive confinement is mobilized, the stress-strain response of the CFRP confined specimens coincided to a large extent with the ascending branch of the stress-strain response of the unconfined specimens. However, beyond a strain of about 0.002, during which the effect of confinement is activated with increase in concrete dilation strain, the stress-strain response of the CFRP confined specimens developed a second response stage, characterized by either a gradually descending branch (for the square specimens) or a gradually ascending branch (for the CFRP circular specimens). The slope of the ascending and descending branches was largely dependent on the area of the CFRP confinement. The second stage of behavior continued until rupture of the CFRP sheets associated with increase in lateral strain of the specimens. Rupture of the CFRP sheets gave rise to a third stage of stress-strain response characterized by a sudden and brittle loss of axial load capacity and complete failure of the specimens. It is clear from the results shown in Figure 4 that increasing the area of CFRP confinement (doubling it in this particular study) leads to sizable increases in the axial load capacity and, more importantly, substantial improvement of the ductility of axial failure. The partially confined (SP) and the fully confined (SF) square specimens acquired an increase in axial strength relative to the unconfined control square specimen (SU) of about 9.0% and 18.0%, respectively. The axial strain at which the CFRP ruptured and the specimens failed completely in compression was about 0.004 for Specimen SP and 0.01 for SF. At approximately the same axial strain of about 0.002 or slightly more, the partially confined (CP) and the fully confined (CF) circular specimens acquired increases in axial strength relative to the unconfined circular specimen (CU) of about 11.5% and 22.0%, respectively. However, at the maximum rupture strain of 0.0078 for Specimen CP and 0.019 for CF, the specimens (CP and CF) acquired increases in axial strength relative to CU of about 21.5% and 44%, respectively.

Figure 3. Typical failure modes of specimens: a) Confined - b) Unconfined

3.2. Cyclic response

As shown from the results depicted in Fig. 4, the cyclic axial stress-strain response can be divided into three distinct paths: a 1st unloading path characterized by a quick and linear drop in axial stress, a 2nd unloading path characterized by a progressively diminishing slope until reaching zero axial stress, and a reloading path characterized by an almost linear stress-strain behavior up to a point on the envelope curve close to the point where unloading occurred. The following interesting observations, which are common to the square and circular specimens tested in this investigation, can be derived from the cyclic responses: (i) the slope of the 1st

unloading path at all strain levels is almost equal to the slope of the envelope stress-strain response during the first elastic stage; (ii) the axial stress at which the 2nd unloading path starts is to some extent proportional to the axial stress on the envelope curve at which unloading initiated, regardless of the axial strain level; and (iii) the slope of the 2nd unloading path and also the slope of the linear reloading path decrease progressively with increase in axial strain.

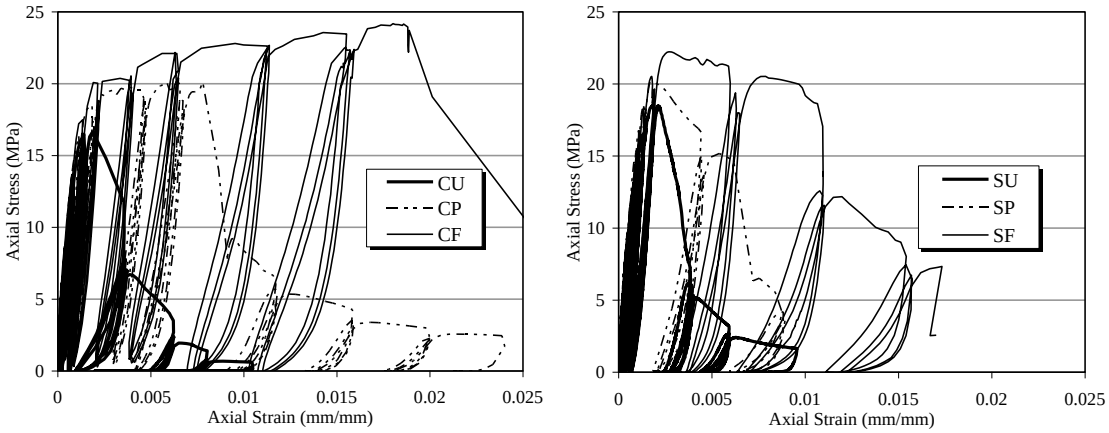

Figure 4. Stress-strain response of the tested circular and square specimens

4. Comparison with existing models

4.1. Model parameters

Previous studies have shown that the envelope axial stress-strain curve of a specimen subjected to cyclic loading is almost identical to the stress-strain curve of the same specimen subjected to monotonic loading [10, 14]. The experimental results shown in Figure 4 can be idealized as shown in Figure 5. This idealization is consistent with Lam and Teng [1, 13] monotonic and cyclic axial stress-strain models for CFRP confined circular columns. It is also consistent with the one developed by Wang et al. [16,18] for predicting the envelope and the cyclic axial stress-strain response of square and circular columns, respectively. In this idealization, the envelope stress-strain curve is divided into the following two distinct stages: a first stage of elastic response up to a transition point at which $\sigma_c = f'_t$ and $\varepsilon_c = \varepsilon_t$, and a second stage extending from the transition point to the ultimate point when the CFRP ruptures, which is referred to as $\sigma_c = f'_{cc}$ and $\varepsilon_c = \varepsilon_{cc}$. Figure 5 shows also the parameters of the unloading cycle. The terms σ_{un} and ε_{un} on the curve correspond to the stress and strain at which unloading occurs. The value of the strain corresponding to a zero stress during unloading is the plastic strain ε_{pl}. For the reloading branch, the load can be removed before the reloading path meets the envelope curve resulting in an internal cycle. When the reloading cycle reaches the envelope curve, the cycle is defined as an envelope cycle. The point where the reloading curve meets the envelope curve is the returning point of coordinates $(\varepsilon_{ret}, \sigma_{ret})$.

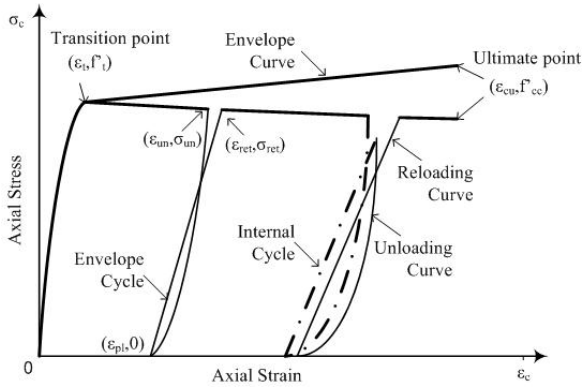

Figure 5. Envelope and cyclic model parameters

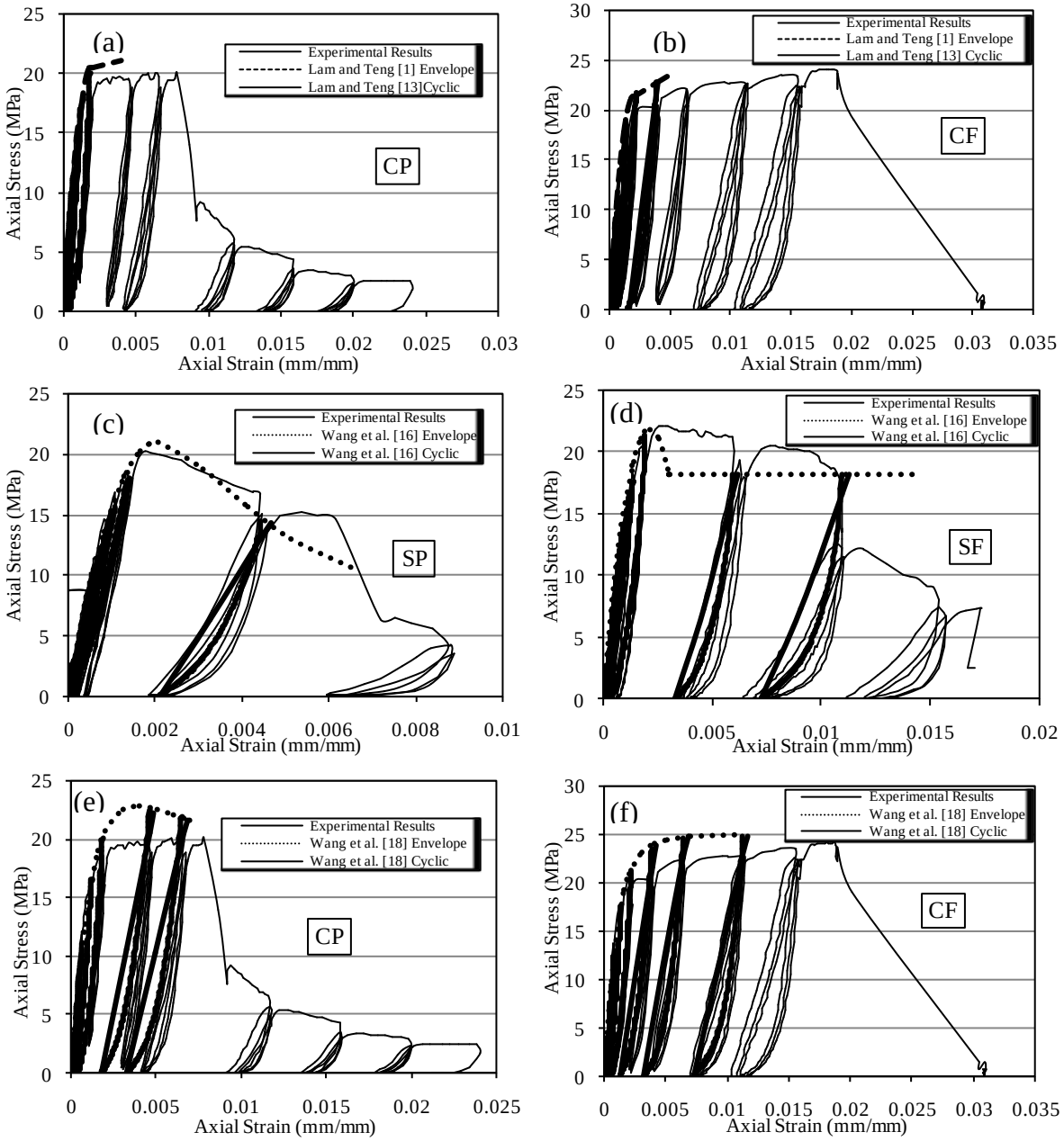

Figure 6. Experimental results and predictions of existing stress-strain models

Figures 6(a) and 6(b) show comparisons between the test results and the response predicted by Lam and Teng model [1, 13] for the two circular column specimens. Figures 6(c) through 6(f) show comparisons between the test results and the predictions of the analytical model proposed by Wang et al. [16, 18] for the square and circular specimens, respectively. For clarity in comparison, the cyclic response of only one cycle predicted by the models was plotted at each strain level. It can be seen in Figures. 6(a) and 6(b) that the model proposed by Lam and Teng predicts the elastic or first stage of the response with good accuracy, but it overestimates the transition stress f'_t. Also, while the corresponding model predicts the ultimate stress f_{cc} with reasonable accuracy, particularly for Specimen CF, it underestimates considerably the ultimate strain ε_{cc}. Within the range of strains predicted by the envelope response, the model predicts the cyclic response reasonably well but this accuracy cannot be verified at the relatively larger strains developed by the circular specimens in this investigation. The models proposed by Wang et al. predict the first elastic stage of the envelope response with a level of accuracy similar to that of Lam and Teng model. While the model predicts with very good accuracy the stress and strain corresponding to the transition point for the square specimens, it tends to overestimate the same for the circular specimens. It is clear from the comparisons shown in Figures 6 that, while the analytical models proposed by Wang et al. predict the overall envelope and cyclic response with reasonable accuracy and better than the model proposed by Lam and Teng, discrepancies still exist between the corresponding models and the test results, particularly in predicting the various characteristic points of the general response given in Figure 5. More test results generated from the current study will be used for further verification of the accuracy of different exiting models and for either generating more accurate models or for refining existing ones.

5. Conclusions

In this paper, the stress-strain response of a limited number of plain concrete column specimens having circular or square cross-sections and subjected to cyclic loading was experimentally investigated. The following conclusions can be drawn:

1) The intrinsic shape of the axial stress-strain response was almost identical for all specimens, regardless of the type of section (circular or square) or area of external CFRP reinforcement.

2) The confinement provided by the CFRP wraps increased the axial strength and resulted in significant improvement of the ductility of axial failure. For the same area of external CFRP reinforcement, the CFRP confinement was more effective for the circular specimens than for the square specimens, as expected.

3) The cyclic axial stress-strain response can be divided into three distinct paths: a 1st unloading path characterized by a quick and linear drop in axial stress, a 2nd unloading path characterized by a progressively diminishing slope until reaching zero axial stress, and a reloading path characterized by an almost linear stress-strain behavior up to a point on the envelope curve close to the point where unloading occurred.

4) Comparisons made between the test results and the predictions of available CFRP confinement models showed that existing models are capable of capturing the global axial stress-strain behavior of the tested specimens. However inaccuracies still existed in predicting the characteristic points of the envelope and cyclic responses.

5) Further test results, which will be generated from the current ongoing experimental study, will be used for either developing a more accurate model or for refining existing models for better prediction of the test results generated in this investigation and other test data reported in the technical literature.

References

[1] L. Lam and J. G. Teng. Design-oriented stress-strain model for FRP-confined concrete. *Constr Build Mater*, 17(6-7):471-489, 2003.

[2] L. Lam and J. G. Teng. Design-oriented stress-strain model for FRP-confined concrete. in rectangular columns. *Journal of Reinforced Plastics and Composites*, 22(13):1149-1186, 2003.

[3] M. Harajli, E. Hantouche and K. Soudki. Stress-strain model for fiber-reinforced polymer jacketed concrete columns. *ACI Structural Journal,* 103(5):672-682, 2006.

[4] T. Rousakis, A. Karabinis and P. Kiousis. FRP-confined concrete members: Axial compression experiment and plasticity modeling. *Eng Struct*, 29:1343 –1353, 2007.

[5] M. Youssef, M. Feng and A. Mosallam. Stress-strain model for concrete confined by FRP composites. *Composites Part B*, 38(5-6):614-628, 2007.

[6] A. Ilki, O. Peker, E. Karamuk, C. Demir and N. Kumbassar. FRP retrofit of low and medium strength circular and rectangular reinforced concrete columns. *J Mater Civ Eng*, 20(2):369-188, 2008.

[7] R. Eid and P. Paultre. Analytical model for FRP-confined circular reinforced concrete columns. *J Compos Constr*, 12(5):541-552, 2008.

[8] B. Csuka and L. Kollar. FRP-confined circular concrete columns subjected to concentric loading. *Journal of Reinforced Plastics and Composites*, 29(23):3504–3520, 2010.

[9] Y. Shao, S. Aval and A. Mirmiran. Fiber-element model of cyclic analysis of concrete-filled fiber reinforced polymer tubes. *J Struct Eng ASCE*, 131(2):292–303, 2005.

[10] M. Harajli, E. Hantouche and K. Soudki. Stress-strain model for fiber-reinforced polymer jacketed concrete columns. *ACI Structural Journal,* 103(5):672-682, 2006.

[11] L. Lam, J. G. Teng, C. H. Cheung and Y. Xiao. FRP-confined concrete under axial cyclic compression. *Cem Concr Res*, 28(10):949-958, 2006.

[12] J. Sakai and K. Kawashima. Unloading and reloading stress–strain model for confined concrete. *J Struct Eng ASCE*, 132(1):112–22, 2006.

[13] L. Lam and J.G. Teng. Stress-strain model for FRP-confined concrete under cyclic axial compression. *Eng Struct*, 31(2):308-321, 2009.

[14] R. Abbasnia and H. Ziaadiny. Behavior of concrete prisms confined with FRP composites under axial cyclic compression. *Eng Struct*, 32(3):648-655, 2010.

[15] Z. Wang, D. Wang, S. Smith and D. Lu. CFRP-confined square RC columns. I: Experimental investigation. *J Compos Constr*, 36(2):150-360, 2012.

[16] Z. Wang, D. Wang, S. Smith and D. Lu. CFRP-confined square RC columns. II: Cyclic axial compression stress-strain model. *J Compos Constr*, 36(2):361-170, 2012.

[17] R. Abbasnia, R. Ahmadi and H. Ziaadiny. Effect of confinement level, aspect ratio and concrete strength on the cyclic stress-strain behavior of FRP-confined concrete prisms. *Composites Part B*, 43:825-831, 2012.

[18] Z. Wang, D. Wang, S. Smith and D. Lu. Experimental testing and analytical modeling of CFRP-confined large circular RC columns subjected to cyclic axial compression. *Eng Struct*, 40:64-74, 2012.

[19] R. Abbasnia, F. Hosseinpour, M. Rostamian and H. Ziaadiny. Effect of corner radius on stress-strain behavior of FRP confined prisms under axial cyclic compression *Eng Struct,* 40:529–535, 2012.

[20] R. Abbasnia and A. Holakoo. An investigation of stress-strain behavior of FRP-confined concrete under cyclic compressive loading. *International Journal of Civil Engineering*, 10(3): 201-209, 2012.

[21] R. Abbasnia, F. Hosseinpour, M. Rostamian and H. Ziaadiny. Cyclic and monotonic behavior of FRP confined concrete rectangular prisms with different aspect ratios. *Constr Build Mater*, 40:118–125, 2013.